



## Amino acid-specific isotopic labeling and active site NMR studies of iron(II)- and iron(III)-superoxide dismutase from *Escherichia coli*

David L. Sorkin<sup>a</sup> & Anne-Frances Miller<sup>b</sup>

<sup>a</sup>Department of Chemistry, The Johns Hopkins University, Baltimore, MD 21218, U.S.A.

<sup>b</sup>Department of Chemistry, University of Kentucky, Lexington, KY 40506-0055, U.S.A.

Received 23 February 2000; Accepted 23 May 2000

**Key words:** active site, assignments, Fe, non-heme iron, paramagnetic, redox, superoxide dismutase

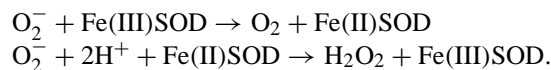
### Abstract

We have developed and employed multiple amino acid-specific isotopic labeling schemes to obtain definitive assignments for active site <sup>1</sup>H NMR resonances of iron(II)- and iron(III)-superoxide dismutase (Fe(II)SOD and Fe(III)SOD) from *Escherichia coli*. Despite the severe relaxivity of high-spin Fe(III), we have been able to assign resonances to ligand His' δ1 protons near 100 ppm, and β and α protons collectively between 20 and 50 ppm, in Fe(III)SOD. In the reduced state, we have assigned all but 7 ligand protons, in most cases residue-specifically. A pair of previously unreported broad resonances at 25.9 and 22.1 ppm has been conclusively assigned to the β protons of Asp 156, superseding earlier assignments (Ming et al. (1994) *Inorg. Chem.*, **33**, 83–87). We have exploited higher temperatures to resolve previously unobserved ortho-like ligand His proton resonances, and specific isotopic labeling to distinguish between the possibilities of δ2 and ε1 protons. These are the closest protein protons to Fe(II) and therefore they have the broadest (~4000 Hz) and most difficult to detect resonances. Our assignments permit interpretation of temperature dependences of chemical shifts, pH dependences and H/D exchange rates in terms of a hydrogen bond network and the Fe(II) electronic state. Interestingly, Fe(II)SOD's axial His ligand chemical shifts are similar to those of the axial His ligand of *Rhodospseudomonas palustris* cytochrome *c'* (Bertini et al. (1988) *Inorg. Chem.*, **37**, 4814–4821) suggesting that Fe(II)SOD's equatorial His<sub>2</sub>Asp<sup>-</sup> ligation is able to reproduce some of the electronic, and thus possibly chemical, properties of heme coordination for Fe<sup>2+</sup>.

**Abbreviations:** Asp, aspartate; FeSOD, iron-containing superoxide dismutase; His, histidine; NOE, nuclear Overhauser effect; NOESY, 2D nuclear Overhauser spectroscopy; Tyr, tyrosine; WEFT, water-eliminated Fourier transform; INEPT, insensitive nuclei enhanced by polarization transfer; DSS, sodium 2,2'-dimethyl-2-silapentane-5-sulfonate; HEPES, N-(2-hydroxyethyl) piperazine-N'-(2-ethanesulfonic acid); IPTG, isopropyl-β-D-thiogalactopyranoside.

### Introduction

Fe-containing superoxide dismutase (FeSOD) catalyzes the disproportionation of O<sub>2</sub><sup>-</sup> to O<sub>2</sub> and H<sub>2</sub>O<sub>2</sub> by the following cyclic mechanism:



\*To whom correspondence should be addressed. E-mail: afm@pop.uky.edu

*Supplementary material:* The individual assignments are available from the authors.

This enzyme is a member of the class of non-heme, non-sulfur mononuclear Fe proteins which includes lipoyxygenase, isopenicillin N synthase and 2,3-dihydroxybiphenyl 1,2-dioxygenase (Feig and Lippard, 1994; Que and Ho, 1996). EPR and optical spectrophotometry of Fe<sup>3+</sup> as well as other methods provide rich information as to the state of the metal ion and its interactions with substrate analogs. In order to understand the interactions between the protein and the metal ion, as well as between the protein and the substrate, we also need spectroscopic probes

of the protein. NMR is ideally suited by its applicability in solution under turnover conditions and its compatibility with titrations.

*E. coli* FeSOD is a 42 kDa homodimer, each monomer of which contains a single Fe ion coordinated in a trigonal bipyramidal geometry by the  $\epsilon 2$  Ns of three His residues (axial His 26 and equatorial His 73 and His 160), equatorial monodentate Asp 156, and one axial solvent molecule, at neutral pH in both oxidation states (Lah et al., 1995; Miller and Sorkin, 1997). The Fe coordinated solvent molecule is thought to be water in Fe(II)SOD and hydroxide in Fe(III)SOD (Stallings et al., 1991). A second hydroxide ion coordinates to Fe(III) with a pK of  $\sim 9$  (Fee et al., 1981; Stallings et al., 1991; Tierney et al., 1995) while in Fe(II)SOD an active site pK of 8.5 is observed, but this ionization is ascribed to non-ligand residue Tyr 34 (Sorkin et al., 1997; Sorkin and Miller, 1997). Fe remains high spin above and below these pKs in both oxidation states. Both the above two pH events affect activity by causing  $K_M$  to increase (Bull and Fee, 1985). The protein may also participate directly in additional events that affect activity, including substrate binding in both the oxidized (Fee et al., 1981; Vathyam et al., 2000) and reduced states (Whittaker and Solomon, 1988; Vathyam et al., 2000).

The  $^1\text{H}$  NMR spectrum of Fe(II)SOD was first reported by Ming et al. (1994) who collectively assigned the three ligand His  $\delta 1$  protons and ascribed spin systems to the ligand Asp and a nearby Trp. Fe(II)SOD from *Methanobacterium thermoautotrophicum* has also been observed by  $^1\text{H}$  NMR (Renault and Morgenstren-Badarau, 1999). Unfortunately, the assignments reported encompassed only a few tentative assignments of the ligands and one second sphere residue. Thus, in order to be able to exploit the capabilities of NMR in the study of the interactions between the FeSOD protein and Fe, substrate and inhibitors, as well as catalytically important pH equilibria, many more definitive assignments are needed.

Paramagnetically shifted NMR resonances were among the first biomacromolecular  $^1\text{H}$  NMR resonances studied in detail (Redfield and Gupta, 1971). However, they are often challenging to assign because wide dispersal of chemical shifts from their characteristic diamagnetic values precludes identification on the basis of chemical shift alone, and fast relaxation rates make multi-dimensional experiments difficult or impossible (but see for example (LaMar et al., 1973; Bertini and Luchinat, 1986; Cheng and Markley, 1995). In favorable cases (line widths  $< \sim 1000$  Hz)

2D NOESY and 1D NOE experiments are successful in identifying spin systems (Thanabal and La Mar, 1989), but multiple amino acid residues may have the same type of spin system. For example, the  $\alpha$ ,  $\beta$ ,  $\beta'$  proton spin system occurs for possible ligand residues His, Asp, Asn, Tyr, Ser, and Cys. Although small molecule model compounds (Lauffer et al., 1983; Wu and Kurtz, 1989) and previously assigned proteins suggest ranges of chemical shifts for these ligands, these ranges overlap and it is possible for compounds to exist that do not fall in the previously observed range. Amino acid-specific isotopic labeling provides unambiguous identification of residue type (Wüthrich, 1969; Weiss et al., 1986; Sadek et al., 1993). We have utilized this technique to obtain  $^1\text{H}$  NMR assignments of Fe(II) and Fe(III)SOD that could not be accurately made using other methods.

Line widths and relaxation rates are also useful tools in assigning paramagnetically shifted resonances (Bertini and Luchinat, 1986; Thanabal and La Mar, 1989). Line width ( $1/T_2$ ) is proportional to  $1/r^6$  (where  $T_2$  is the transverse relaxation time and  $r$  is the distance from the resonating nucleus to the metal ion) when dipolar (including Curie) relaxation prevails. Curie relaxation (Gueron, 1975) is the dominant paramagnetic mechanism for proton relaxation in Fe(II)SOD (Lansing and Miller, unpublished). Hyperfine and ligand centered dipolar relaxation may make ligand resonances somewhat broader than those of equidistant non-ligand protons. Nonetheless, the distance dependence of line width is extremely useful for assigning resonances of proteins for which the structure is known (Satterlee, 1986). If some paramagnetically shifted resonances are assigned and their line widths measured, a distance versus line width calibration curve can be established. Expected resonance line widths for unassigned protons can then be calculated based upon their distances to the metal ion, establishing a criterion for assignment.

We have combined exceptionally clean isotopic labeling with 1D NOE,  $^1\text{H}$ - $^{15}\text{N}$  INEPT and 2D NOESY spectra, as well as consideration of line widths and H/D exchangeability. Thus, we now report 19 new Fe(II)SOD resonance assignments including some for resonances which have not previously been detected, and several which correct previous assignments. We also report the first assignments of the poorly resolved Fe(III)SOD  $^1\text{H}$  NMR spectrum. These assignments will enable the effects of exogenous ligand binding and amino acid ionization and mutation to be analyzed in terms of specific FeSOD protons. To our knowl-

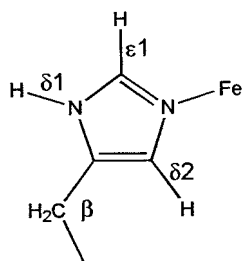
edge, this work represents the most complete set of metal site  $^1\text{H}$  NMR assignments for a member of the class of mononuclear high spin non-heme, non-sulfur Fe enzymes.

## Experimental

**Isotopic labeling.** While all FeSOD samples were purified from *E. coli* as described previously (Sorkin and Miller, 1997), the growth conditions for each labeling scheme varied as follows:

Unlabeled (Sorkin and Miller, 1997) and  $^{15}\text{N}$  FeSOD (Vance et al., 1997) were prepared as previously described.

$[\epsilon 1\text{-}^2\text{H}]$  His FeSOD was purified from *E. coli* BL21 bearing the overexpression plasmid pRLK3 (Vathyam et al., 1999) grown aerobically in M9 media, to which 400 mg/l  $[\epsilon 1\text{-}^2\text{H}]$  L-His was added. This labeling method was previously shown to be successful without the use of an auxotrophic strain (Browne et al., 1973; Banci et al., 1990; Pappu and Serpersu, 1994). The addition of  $[\epsilon 1\text{-}^2\text{H}]$ -L-His was delayed until  $\text{OD}_{600} = 0.2$  (7 h prior to harvest) to minimize solvent exchange of the label which occurs with a half-life of 56 h at pH 7.6 at 37 °C. Expression was induced with 1 mM final concentration of IPTG added at  $\text{OD}_{600} = 1.0$ , and harvesting followed 4 h later. Following the example of imidazole studies (Vaughan et al., 1970)  $[\epsilon 1\text{-}^2\text{H}]$ -L-histidine was made by heating pD 10 L-His in  $^2\text{H}_2\text{O}$  for 16 h at 73 °C.



$[\epsilon 1, \delta 2\text{-}^2\text{H}]$  His FeSOD was produced the same way as  $[\epsilon 1\text{-}^2\text{H}]$  His FeSOD, except by using  $[\epsilon 1, \delta 2\text{-}^2\text{H}]$ -L-histidine, which was made by heating flame sealed ampoules of L-His dissolved in  $^2\text{H}_2\text{O}$  with 1 M  $\text{NaO}^2\text{H}$  at 121 °C for 2 h.

$[\delta 2\text{-}^2\text{H}]$  His FeSOD was produced the same way as was  $[\epsilon 1\text{-}^2\text{H}]$  His FeSOD, except by using  $[\delta 2\text{-}^2\text{H}]$ -L-histidine which was made by heating pH 10  $[\epsilon 1, \delta 2\text{-}^2\text{H}]$ -L-histidine in  $^1\text{H}_2\text{O}$  for 16 h at 73 °C.

$^1\text{H}$  His  $^2\text{H}$  FeSOD was purified from *E. coli* BL21 with plasmid pRLK3 (Vathyam et al., 1999) grown aerobically in M9 media made with > 98%  $^2\text{H}_2\text{O}$ , using 0.2% v/v  $^2\text{H}$  glycerol as the main carbon source and containing 200 mg/l L-histidine. The addition of L-His was postponed until  $\text{OD}_{600} = 0.2$  (11 h prior to harvest) to minimize solvent exchange of the  $\epsilon 1$  position. Expression was induced at  $\text{OD}_{600} = 1.0$  and cells were harvested 4 h later.

$^2\text{H}$  Asp FeSOD was overexpressed using *E. coli* auxotrophic strain JK120 (Parker and Friesen, 1980) containing plasmid pHS1-8 (Carlioz et al., 1988) grown anaerobically in defined media containing 400 mg/l  $^2\text{H}$  D-L-aspartate (Hu and Redfield, 1993) but otherwise the same as that of Muchmore et al. (1989) except containing half the concentrations of bases and amino acids and 10 times the concentrations of micronutrients.

$^1\text{H}$  Asp  $^2\text{H}$  FeSOD was purified from *E. coli* BL21 with plasmid pRLK3 (Vathyam et al., 1999) grown aerobically in M9 media made with > 98%  $^2\text{H}_2\text{O}$ , using 0.2% v/v  $^2\text{H}$  glycerol as the main carbon source and containing 200 mg/l of L-aspartate and 125 mg/l of L-methionine. The addition of methionine and aspartate was delayed until  $\text{OD}_{600} = 0.8$  to minimize leak of protons from aspartate to other amino acids. L-methionine was added to suppress the production of threonine and lysine from aspartate. FeSOD contains no Met. Expression was induced 20 min later and harvesting occurred 2 h after induction.

$^1\text{H}$  Tyr  $^2\text{H}$  FeSOD was purified from *E. coli* QC774 with plasmid pHS1-8 (Carlioz et al., 1988) grown anaerobically in M9 media made with > 98%  $^2\text{H}_2\text{O}$  and 88 mg/l L-tyrosine using 0.3%  $^2\text{H}$  acetic acid as the carbon source. We find that using  $^2\text{H}$  glycerol as a carbon source is a much more reliable method of growing *E. coli* in  $^2\text{H}_2\text{O}$  than using  $^2\text{H}$  acetic acid.

**NMR spectroscopy.** All data were collected on a Bruker AMX300 spectrometer at 303 K unless otherwise noted. FeSOD samples contained no buffers or salts unless specifically indicated and were reduced, after degassing, with sodium dithionite in 0.1 M NaOH and flame sealed in NMR tubes unless otherwise noted. pHs were determined by the use of internal indicator molecules' chemical shifts from internal DSS as previously described (Sorkin and Miller, 1997). The pD of  $^2\text{H}_2\text{O}$  solutions was also determined using these indicators without correction for isotope effects and is designated by the symbol pH\*.

The super-WEFT (Inubishi and Becker, 1983) pulse sequence used to observe [ $^1\text{H}$ ] Asp [ $^2\text{H}$ ] Fe(II)SOD contained no relaxation delay, a 9 ms delay following the  $180^\circ$  pulse and a 10 ms acquisition time. No water presaturation was used. All other super-WEFT sequences contained a 15 ms relaxation delay, a 35 ms delay between pulses and a 25 ms acquisition time. Water was saturated during both delays.

1D NOE difference spectra were collected in interleaved blocks of 240 transients. Each transient contained a 200 ms delay during which water and another frequency were irradiated, followed by a  $90^\circ$  pulse and 50 ms acquisition time. A spectrum collected with a resonance of interest 75% saturated was subtracted from another spectrum collected using the same power of saturation applied the same number of Hz to the other side of the resonance nearest the one being saturated in the first scan. Alternately, if there was no evidence of saturation of the closest resonance to the one being saturated, the experimental spectrum was subtracted from one obtained with off-resonance saturation, the same number of Hz from the water resonance but on the other side of it.

NOESY spectra consisted of 1514 points in the direct dimension and 256 in the indirect dimension. Water was saturated during the 200 ms relaxation delay and during the mixing time. Three NOESYs were collected, with mixing times of 7, 15, and 30 ms, and acquisition times of 50 ms in all cases.

Reverse ( $^{15}\text{N}$  to  $^1\text{H}$ ) INEPT spectra were acquired both with and without refocusing, but in all cases without decoupling. An acquisition time of 25 ms and a relaxation delay of 500 ms were used. Water was saturated during all delays.

For the purpose of measuring exchange rates, solvent exchange was initiated by repeated concentration and dilution with  $^2\text{H}_2\text{O}$  of Fe(III)SOD, at pH 6.0 to minimize premature exchange, in Centricon ultrafilters. Four cycles of concentration and dilution by a factor of four with  $^2\text{H}_2\text{O}$  were used to obtain >99%  $^2\text{H}_2\text{O}$ . Samples were then reduced in valve and septum sealed NMR tubes and the pD was increased to the desired value by injecting 0.1 M  $\text{NaO}^2\text{H}$ . Super-WEFT spectra were then acquired over a period of 116 h for the pH\* 7.0 sample and 24 h for pH\* 7.8.

Distances of protons from Fe were obtained using the Fe(II)SOD X-ray crystal structure coordinates of Lah et al. (1995) and the Biosym InsightII molecular modeling program. Distances are quoted to tenths of Å in accordance with the precision of  $\pm 0.3$  Å expected

from the 1.8 Å resolution crystal structure, with the caveat that the solution structure may differ slightly.

## Results

At first glance, the paramagnetically shifted resonances of Fe(II)SOD appear well resolved (Figure 1). However, by examining the pH (Sorkin and Miller, 1997) and temperature dependence of the Fe(II)SOD  $^1\text{H}$  NMR spectrum, as well as through isotopic labeling, additional paramagnetically shifted resonances are revealed, demonstrating that the spectrum is a highly overlapped collection of resonances. For example, in the 20–27 ppm range we find a total of at least six resonances. As the pH is increased above the active site pK of 8.5, the sharp resonance **e** shifts downfield revealing a broader, less pH dependent, feature (Figures 2A and 2B). This feature is composed of two resonances, one solvent exchangeable (**e'**) and one non-exchangeable (**e''**)<sup>1</sup>. The existence of the exchangeable proton was confirmed by observing [ $^1\text{H}$ ] Tyr [ $^2\text{H}$ ] Fe(II)SOD in  $^1\text{H}_2\text{O}$  versus  $^2\text{H}_2\text{O}$ . In spectra of [ $^1\text{H}$ ] Tyr [ $^2\text{H}$ ] Fe(II)SOD in  $^1\text{H}_2\text{O}$ , **f** and **e'** are observed (Figure 2C), but upon transfer to  $^2\text{H}_2\text{O}$  **e'** rapidly and **f** slowly disappear, leaving no resonances in the 20–27 ppm range (data not shown). On the other hand, the existence of the non-exchangeable resonance **e''** is confirmed by its presence in spectra of Fe(II)SOD in  $^2\text{H}_2\text{O}$  at high pH (Figure 2D). Additionally, two broader resonances are found at 26 and 22 ppm (not lettered in Figure 2, see Figures 1 and 8), which are obscured by the overlapping sharper resonances in unlabeled FeSOD. These resonances are discussed in detail below. Resonances in other portions of the spectrum are similarly overlapped, such as **j'**, which overlaps **j** and **k** at low pH, and **i** at high pH while being observed in isolation near pH 8.5 at 16 ppm (see Figure 2 in Sorkin and Miller (1997)). Thus, many more protons have shifted resonances than might be guessed, and the paramagnetic spectrum must encompass many second-sphere residues. Hence it is a valuable probe of the residues that modulate the chemistry of the active site but are difficult to assign by reference to model compounds.

<sup>1</sup>We use the symbol ' to designate previously unreported resonances for downfield resonances a–p so as to maintain the lettering system of Ming et al. (1994); however, we have adopted the letters r–z for upfield resonances.

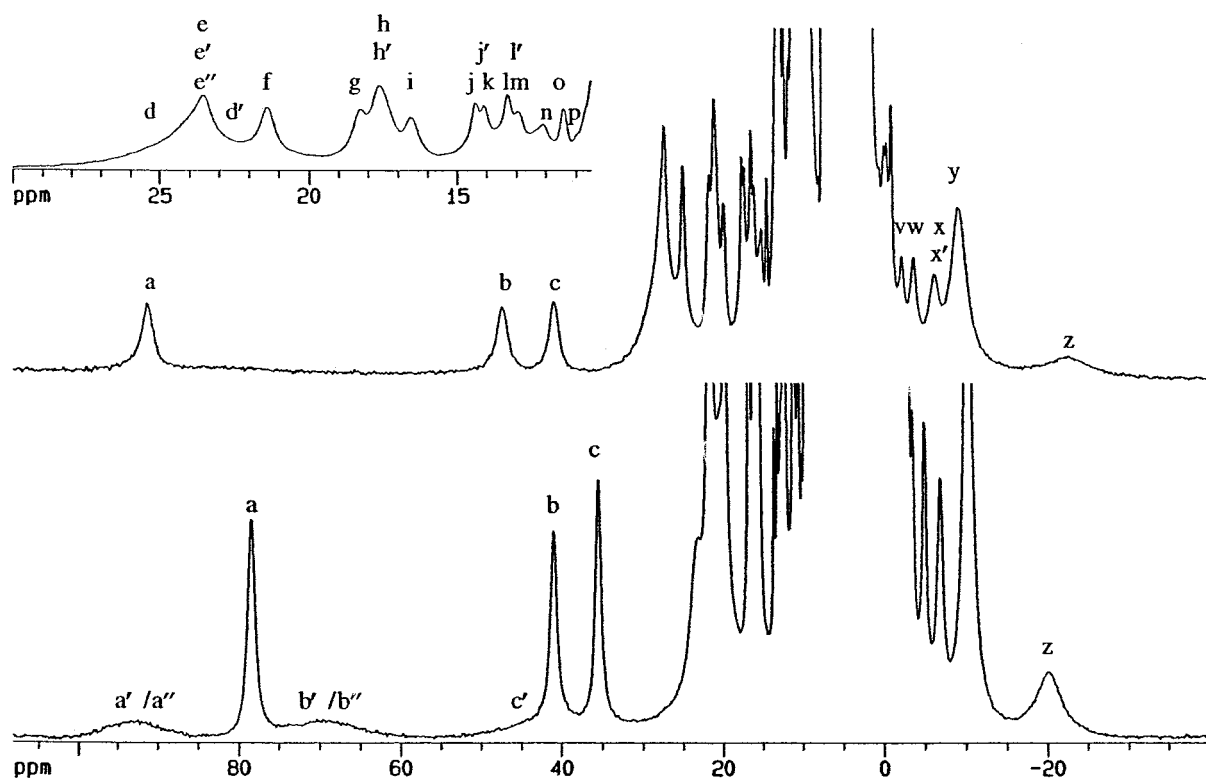


Figure 1.  $^1\text{H}$  NMR super-WEFT spectra (300 MHz) of unlabeled Fe(II)SOD in 90%  $^1\text{H}_2\text{O}/10\%$   $^2\text{H}_2\text{O}$ , pH 7.0, with 50 mM HEPES and 100 mM NaCl at 30  $^\circ\text{C}$  (top and inset) and 50  $^\circ\text{C}$  (bottom).

**Solvent exchange of Fe(II)SOD protons.** As a first step towards assigning and resolving the many resonances in Fe(II)SOD's spectrum we classified them according to solvent exchangeability, and thus chemical type. In addition to the four resonances **a**, **b**, **c**, and **f**, which were reported to be exchangeable by Ming et al. (1994), we also find **e'**, **i**, **j**, **j'**, **n**, and **p** to be exchangeable.  $^{15}\text{N}$ - $^1\text{H}$  reverse INEPT shows **f**, **i**, **j**, **k**, **n**, **p**, and **x** to be resonances of NH protons (data not shown) and thus resonances of His, Gln, Asn or Trp side chains, or backbone NHs<sup>2</sup>. Reverse INEPT is used because the relaxation times of  $^{15}\text{N}$  are much longer than those of  $^1\text{H}$ , making it advantageous to transfer from  $^{15}\text{N}$  and digitize  $^1\text{H}$ . Nonetheless, resonances **a**, **b**, **c**, **e'**, and **j'** were unobservable in the reverse INEPT spectra, probably due to their fast relaxation rates.

<sup>2</sup>The solvent exchange rates of **k** and **x** are immeasurably slow. The exchange rates of protons **f**, **i**, **j** were measured by observing decreases in resonance intensity upon exchange of Fe(II)SOD into  $^2\text{H}_2\text{O}$ . The exchange rates are  $0.0327 \pm 0.0007$ ,  $0.090 \pm 0.002$ , and  $0.0328 \pm 0.0014 \text{ h}^{-1}$  at pH\* 7.0 and  $0.111 \pm 0.009$ ,  $0.34 \pm 0.02$ , and  $0.151 \pm 0.011 \text{ h}^{-1}$  at pH\* 7.8, respectively.

**Ligand His assignments of Fe(II)SOD.** The ligand His  $\delta 1$  protons provide a convenient entry-point from which to assign the other ligand His protons. To unambiguously identify protons of histidines,  $[\text{H}]$  His  $[\text{H}]$  FeSOD was produced. This sample produces  $^1\text{H}$  spectra containing only the resonances of histidines and thus both minimizes spectral complexity and overlap, but also identifies any resonances visible as those of His (when the sample contains only  $^2\text{H}_2\text{O}$ ). Resonances **a**, **b**, and **c** are the three ligand His  $\delta 1$  proton resonances (Ming et al., 1994). NOE difference spectra of unlabeled and  $[\text{H}]$  His  $[\text{H}]$  Fe(II)SOD in  $^1\text{H}_2\text{O}$  allowed each ligand His  $\delta 1$  proton to be linked to its corresponding  $\beta$ ,  $\beta'$  pair (Figure 3, also see below). By partially saturating peak **a**, NOEs to **e**, **g**, and **j** were observed, as well as NOEs to non-His peaks **k**, **h** (and/or **h'**), and **o**. When peak **b** of  $[\text{H}]$  His  $[\text{H}]$  FeSOD was partially saturated, NOEs to the  $\beta$  pair **r** and **v** as well as to **u** were obtained. Likewise, NOEs from **c** to **s** and **t** were observed.

NOESY spectra of  $[\text{H}]$  His  $[\text{H}]$  Fe(II)SOD in  $^2\text{H}_2\text{O}$  with mixing times of 7, 15, and 30 ms reveal three strong cross peaks: **e-g**, **s-t**, and **r-v** (Figure 4).

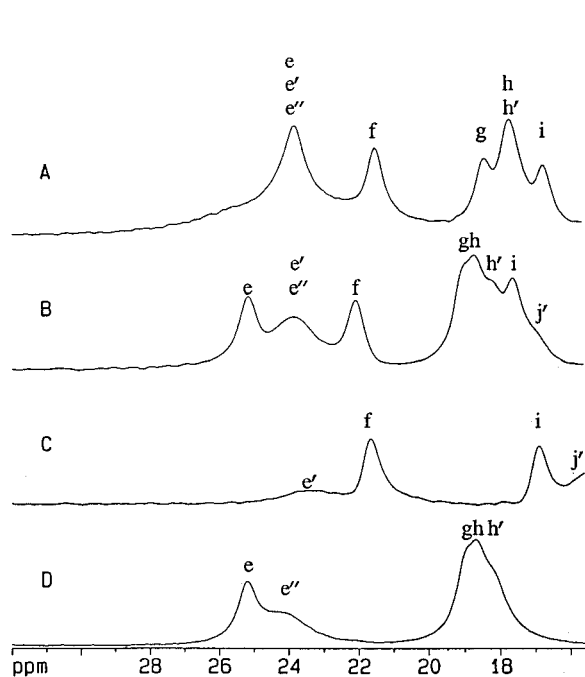


Figure 2.  $^1\text{H}$  NMR super-WEFT spectra ( $30^\circ\text{C}$ , 300 MHz) of unlabeled Fe(II)SOD pH 6.8 in 90%  $^1\text{H}_2\text{O}/10\%$   $^2\text{H}_2\text{O}$  (A), unlabeled Fe(II)SOD pH 10.6 in 90%  $^1\text{H}_2\text{O}/10\%$   $^2\text{H}_2\text{O}$  (B),  $[\text{H}^1]\text{Tyr}$   $[\text{H}^2]\text{Fe(II)SOD}$  pH 8.2 in 90%  $^1\text{H}_2\text{O}/10\%$   $^2\text{H}_2\text{O}$  (C), and unlabeled Fe(II)SOD pH\* 10.5 in  $^2\text{H}_2\text{O}$  (D).

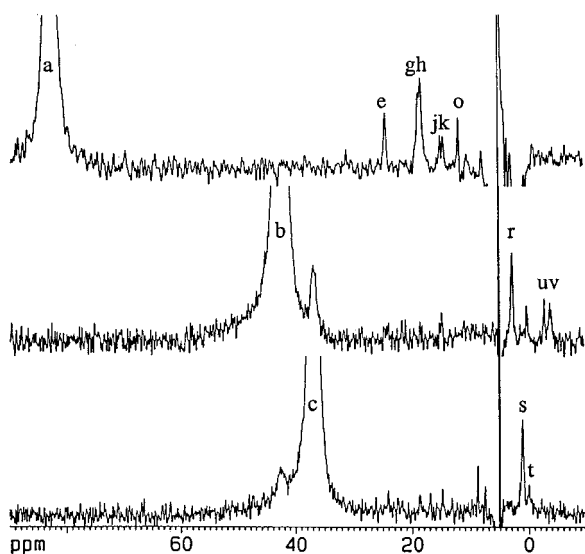


Figure 3.  $^1\text{H}$  NMR NOE difference spectra ( $30^\circ\text{C}$ , 300 MHz, saturation time 200 ms) in  $^1\text{H}_2\text{O}$  of unlabeled Fe(II)SOD with **a** saturated (top),  $[\text{H}^1]\text{His}$   $[\text{H}^2]\text{Fe(II)SOD}$  with **b** saturated (middle), and  $[\text{H}^1]\text{His}$   $[\text{H}^2]\text{Fe(II)SOD}$  with **c** saturated (bottom).

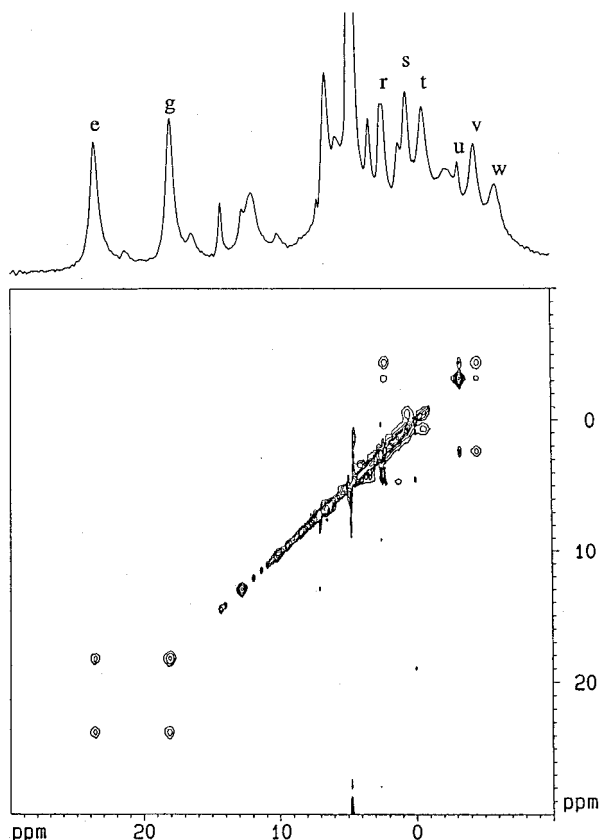


Figure 4.  $^1\text{H}$  NMR ( $30^\circ\text{C}$ , 300 MHz) super-WEFT spectrum (top) and NOESY spectrum with 30 ms mixing time (bottom) of  $[\text{H}^1]\text{His}$   $[\text{H}^2]\text{Fe(II)SOD}$  in  $^2\text{H}_2\text{O}$ .

Each of these six resonances have line widths of  $\sim 160$  Hz, indicating they are approximately equidistant from Fe(II). We collectively assign these cross peaks to the three  $\beta$ ,  $\beta'$  proton pairs of the three ligand His', all of which are between 5.6 and 6.3 Å from Fe(II). These connectivities confirm the proposals based on the 1D NOEs from the ligand His  $\delta 1$  protons.

The possibility that any of the NOESY cross peaks are those of non-ligand His 30 or His 31 is eliminated by consideration of the 1D NOE data, which connects each  $\beta$  pair to a ligand  $\delta 1$  proton, and the fact that no His 30 or 31 protons are within 4 Å of a ligand  $\delta 1$  proton. The  $\beta$  protons of His 30 are closer to iron (4.8 and 5.2 Å) than are the ligand His  $\beta$  protons (5.6 to 6.3 Å), while the  $\beta$  protons of His 31 are at 6.0 and 7.7 Å. Thus, peak w, which is broader than the ligand His  $\beta$  protons is likely that of a His 30  $\beta$  proton, because the closer ligand protons are all accounted for (below) and the His 30  $\beta$  protons are the only non-ligand His

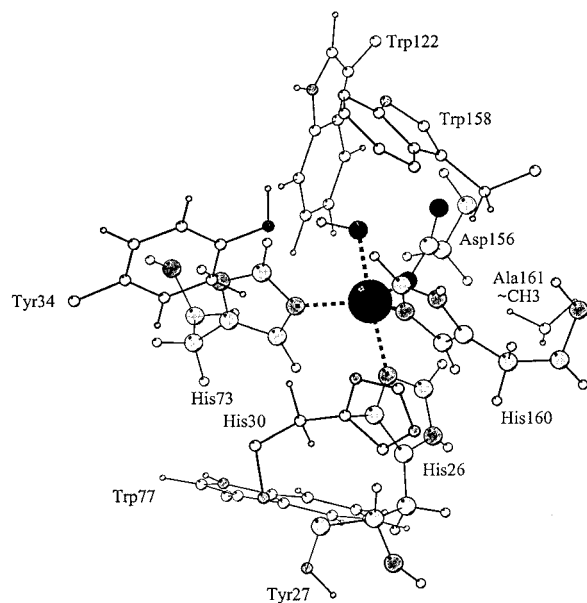


Figure 5. Model of the active site of Fe(II)SOD based on the crystallographic coordinates of Fe(II)SOD (Lah et al., 1995). For simplicity many atoms are not shown, however, all but three residues with an atom within 6 Å of Fe(II) are represented. In particular, H atoms far from Fe(II) and backbone atoms that were not assigned are omitted. To aid in their identification, ligands' atoms are twice as large as those of non-ligands.

protons closer to iron than the ligand His  $\beta$  protons, and therefore the only ones that could have broader resonances.

The relatively sharp (70 Hz) resonance **u** is assigned to a ligand His  $\alpha$  proton based upon its cross peaks with **r** and **v**. The  $\alpha$  protons of His 26 and His 73 are 5.4 and 5.6 Å from Fe(II) and are expected to have line widths similar to those of the ligand His  $\beta$  protons, while that of His 160 is 7.2 Å away and should therefore have a narrower resonance. On this basis we assign **u** to the  $\alpha$  and **r** and **v** to the  $\beta$  protons of His 160 (Table 1). Unassigned paramagnetically shifted resonances in the  $[^1\text{H}]$  His  $[^2\text{H}]$  Fe(II)SOD 1D spectrum may be those of His 30 and 31 protons, the two ligand  $\alpha$  protons unobserved in the NOESY and slowly exchanging protons which were trapped by the protein during purification, when it was exposed to  $^1\text{H}_2\text{O}$ .

Resonances **e** and **g** were previously assigned to the  $\beta$  protons of Asp 156 (Ming et al., 1994). Ming et al. dismissed the possibility that these resonances were those of a ligand His on the basis that "His  $\beta$  protons are found at ca. 10 ppm for  $\epsilon 2$  coordinated residues". However, resonances at 24 and 14 ppm were assigned to the ligand His  $\beta$  protons of high-spin

Table 1. Fe(II)SOD  $^1\text{H}$  NMR assignments

Resonance	Assignment	Chemical shift (ppm)
<b>a</b>	His 26 $\delta$	83.9 <sup>a</sup>
<b>a'/a''</b>	His 73 and 160 $\delta 2$	93 <sup>b</sup>
<b>b</b>	His 160 $\delta 1$	42.5 <sup>a</sup>
<b>b'/b''</b>	His 73 and 160 $\epsilon 1$	70 <sup>b</sup>
<b>c</b>	His 73 $\delta 1$	36.4 <sup>a</sup>
<b>c'</b>	His 26 $\delta 2$	42 <sup>b</sup>
<b>d</b>	Asp 156 $\beta$	25.9 <sup>a</sup>
<b>d'</b>	Asp 156 $\beta$	22.1 <sup>a</sup>
<b>e</b>	His 26 pro-S $\beta$	23.6 <sup>a</sup>
<b>g</b>	His 26 pro-R $\beta$	18.3 <sup>a</sup>
<b>h</b>	Trp 77 $\eta 2$	17.7 <sup>a</sup>
<b>j</b>	His 26 NH	14.5 <sup>a</sup>
<b>k</b>	Tyr 27 NH	14.2 <sup>a</sup>
<b>l'</b>	Tyr 34 $\epsilon$	13.5 <sup>a</sup>
<b>o</b>	Trp 77 $\zeta 3$	11.5 <sup>a</sup>
<b>r</b>	His 160 $\beta$	2.5 <sup>a</sup>
<b>s</b>	His 73 $\beta$	0.7 <sup>a</sup>
<b>t</b>	His 73 $\beta$	-0.5 <sup>a</sup>
<b>u</b>	His 160 $\alpha$	-3.2 <sup>a</sup>
<b>v</b>	His 160 $\beta$	-4.4 <sup>a</sup>
<b>w</b>	His 30 $\beta$	-5.7 <sup>a</sup>
<b>y</b>	Ala 161 $\beta$	-10.8 <sup>a</sup>
<b>z</b>	Trp 158 $\beta$ or Trp 122 $\eta 2/\zeta 2$	-23.7 <sup>a</sup>

<sup>a</sup>pH 7, 30 °C.

<sup>b</sup>pH 7, 50 °C.

Fe(II) cytochrome *c'* from *Rhodocyclus gelatinosus* (Bertini et al., 1993a) and the analogous resonances of *Rhodopseudomonas palustris* cytochrome *c'* are found at 21 and 14 ppm (Bertini et al., 1998). These chemical shift values are in good agreement with those of **e** (24 ppm) and **g** (18 ppm).

Fe(II)SOD His  $\delta 1$  proton resonance **a** is found at 88, 84, and 81 ppm, **b** at 43, 43, and 42 ppm, and **c** at 36, 36, and 36 ppm at 20, 30 and 40 °C. Resonances **b** and **c** have similar chemical shift values and temperature dependencies, but differ substantially from those of **a** (also see Ming et al. (1994)). Thus we conclude that **a**, and therefore **e** and **g**, correspond to the axial His 26 while **b** and **c**, and therefore **s** and **t**, as well as **r**, **v**, and **u**, are equatorial His protons. The corresponding  $\beta$  protons of these resonances show similar patterns. The chemical shifts of resonances **a**, **e** and **g**, but not **b**, **r** and **v** nor **c**, **s** and **t** agree well with the axial His chemical shift values of some heme proteins. The  $\delta 1$  proton of the axial ligand His has a chemical shift of 94 ppm in *R. palustris* Fe(II) cytochrome *c'* at

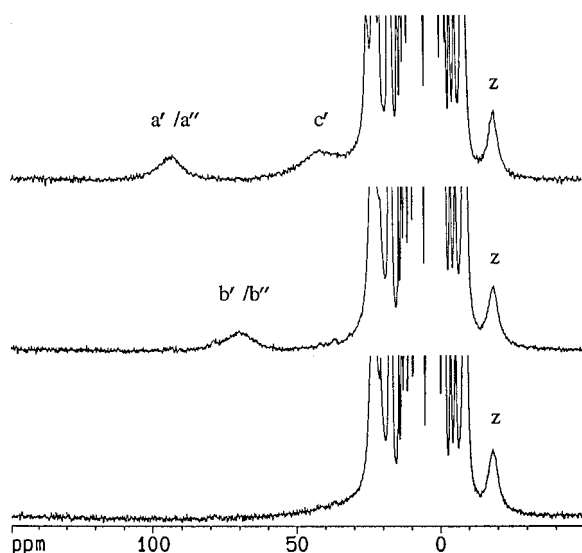


Figure 6.  $^1\text{H}$  NMR super-WEFT spectra (50 °C, 300 MHz) of His labeled Fe(II)SOD in  $^2\text{H}_2\text{O}$ . [ $\epsilon 1\text{-}^2\text{H}$ ] His Fe(II)SOD (top), [ $\delta 2\text{-}^2\text{H}$ ] His Fe(II)SOD (middle), and [ $\epsilon 1, \delta 2\text{-}^2\text{H}$ ] His Fe(II)SOD (bottom). For comparison to unlabeled Fe(II)SOD see the 50 °C spectrum in Figure 1.

25 °C (Bertini et al., 1998), and 75, 76, and 78 ppm in sperm whale, horse and human deoxymyoglobin at 35 °C (Bougault et al., 1998), with values for those of other heme proteins falling in this range (Bertini et al., 1993d). Since we have assigned **b**, **r**, **v**, and **u** to His 160 (above), **c**, **s** and **t** are assigned to the remaining ligand His, His 73 by default.

Resonance **j** was previously assigned to the  $\alpha$  proton of Asp 156 due to reported NOESY cross peaks with **e** and **g** (Ming et al., 1994). We also observe these cross peaks in samples where the solvent is  $^1\text{H}_2\text{O}$ , and in  $^2\text{H}_2\text{O}$  samples before exchange of **j** with solvent is complete; however, our observations that **j** is solvent exchangeable and present in  $^{15}\text{N}\text{-}^1\text{H}$  reverse INEPT spectra preclude its assignment to any  $\alpha$  proton. Resonance **j** is most likely the backbone NH proton of the same ligand His as **a**, **e**, and **g**, His 26. The narrow resonance line width of **j** (90 Hz) is also more consistent with the backbone amide proton of His 26 (7.9 Å from Fe) than the  $\alpha$  proton (5.4 Å). The distances from the two His 26  $\beta$  protons to the  $\alpha$  proton are 2.6 and 3.0 Å, while the distances to the backbone NH proton are 2.3 and 2.7 Å. The intensity of a NOESY cross peak is inversely proportional to  $r^6$ , where  $r$  is the distance between the two nuclei producing the cross peak. Because  $\beta$  protons can be just as close to the backbone NH as to the  $\alpha$  proton and backbone NH protons can

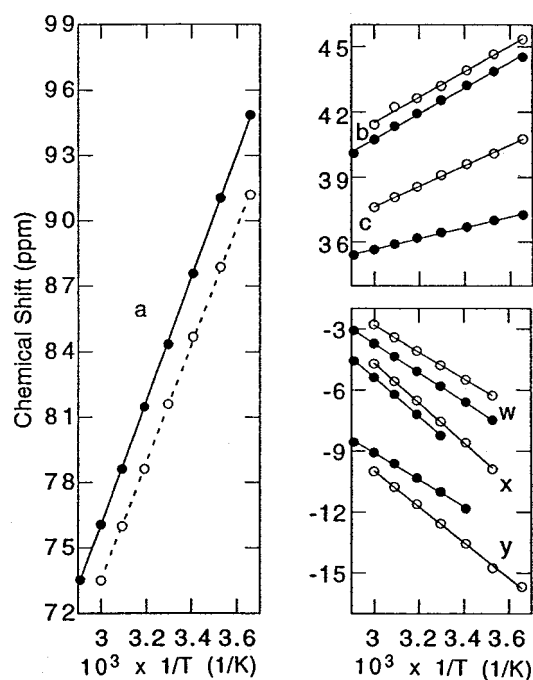


Figure 7. Temperature dependence of the Fe(II)SOD  $^1\text{H}$  NMR spectrum at pH 7.0 (filled circles) and pH 10.1 (open circles). Best fit straight lines are shown: (a) pH 7.0,  $y = -9.3144 + 28.446x$ ,  $R = 0.99995$ , pH 10.1,  $y = -7.5135 + 27.017x$ ,  $R = 0.99993$ ; (b) pH 7.0  $y = 22.905 + 5.9409x$ ,  $R = 0.99878$ , pH 10.1  $y = 24.053 + 5.8273x$ ,  $R = 0.99816$ ; (c) pH 7.0  $y = 28.124 + 4.699x$ ,  $R = 0.9983$ , pH 10.1  $y = 23.563 + 4.699x$ ,  $R = 0.99941$ ; (w) pH 7.0,  $y = 17.61 + -7.1049x$ ,  $R = 0.99996$ , pH 10.1,  $y = 16.91 + -6.5702x$ ,  $R = 0.99995$ ; (x) pH 7.0,  $y = 23.461 + -9.6099x$ ,  $R = 0.9998$ , pH 10.1,  $y = 24.52 + -9.7325x$ ,  $R = 0.99973$ ; (y) pH 7.0,  $y = 10.813 + -6.6309x$ ,  $R = 0.99921$ , pH 10.1,  $y = 16.304 + -8.7619x$ ,  $R = 0.99954$ .

exchange extremely slowly, NOE data is insufficient to distinguish the two cases and additional information such as from  $^{15}\text{N}\text{-}^1\text{H}$  reverse INEPT or COSY spectra is necessary. However, COSY spectra are difficult to interpret in paramagnetic systems as cross peaks can arise due to cross-correlation relaxation effects in addition to true scalar coupling (Bertini et al., 1993b; Qin et al., 1993). We also detect a cross peak between **g** and **k** in NOESY spectra of unlabeled FeSOD (data not shown), but **k** is also an NH proton resonance so the  $\alpha$  proton of His 26 remains unassigned, possibly because its proximity to Fe hinders the detection of a NOESY cross peak. Likewise the  $\alpha$  proton of His 73 is 5.6 Å from Fe(II) and remains unassigned.

*Temperature dependence of Fe(II)SOD.* Although the His 26  $\delta 1$  resonance appears to be the most



strongly shifted resonance in the 30 °C spectrum, the closest Fe(II)SOD protein protons to iron are the six ligand His  $\delta 2$  and  $\epsilon 1$  protons<sup>3</sup> (see below), which are 3.2–3.4 Å from Fe. The corresponding resonances could be more strongly shifted and should also be broader, explaining the difficulty of observing them at room temperature (see also Ming et al. (1994)). At 50 °C three broad ( $\sim 4000$  Hz) features (**a'/a''**, **b'/b''**, and **c'**) are observed and have relative areas of approximately 2:2:1 (Figure 1). These were confirmed to be His  $\delta 2$  and  $\epsilon 1$  protons by their absence in the spectrum of [ $\epsilon 1, \delta 2$ -<sup>2</sup>H] His Fe(II)SOD (Figure 6). Feature **b'/b''** is absent from spectra of [ $\epsilon 1$ -<sup>2</sup>H] His Fe(II)SOD, while **a'/a''** and **c'** are absent from spectra of [ $\delta 2$ -<sup>2</sup>H] His Fe(II)SOD. Feature **b'/b''** is therefore assigned to two ligand His  $\epsilon 1$  protons. Because **b'** and **b''** have nearly identical chemical shifts they are most likely  $\epsilon 1$  resonances of the two equatorial His, His 73 and 160. Likewise feature **a'/a''** is assigned to two equatorial His  $\delta 2$  protons, while **c'** is assigned to the axial His 26  $\delta 2$  proton. A third  $\epsilon 1$  proton resonance, that of His 26, is unobserved, probably due to overlap with sharper resonances. In general,  $\epsilon 1$  proton resonances are found upfield of their corresponding  $\delta 2$  proton resonances for His residues coordinated to high-spin Fe(II) through N $\delta 2$  (Goff and La Mar, 1977; La Mar et al., 1977; Balch et al., 1985; Wu and Kurtz, 1989; Bertini et al., 1998). We therefore expect the  $\epsilon 1$  proton resonance of His 26 to be in the 30 to  $-20$  ppm range, obscured due to resonance overlap.

The temperature dependence of the paramagnetically shifted Fe(II)SOD resonances was investigated above and below the active site pK of 8.5 (Sorkin and Miller, 1997) (Figure 7). At pH 7.0 Fe(II)SOD was stable on the time scale of the experiment until 70 °C was reached and rapid precipitation occurred. At pH 10.1 Fe(II)SOD was stable until 60 °C was reached, and then became gelatinous yet clear instead of precipitating. While some resonances show pH dependence only in the  $1/T = 0$  intercept, others such as ligand His  $\delta 1$  proton resonance **c** also exhibit changes in the slope. The latter demonstrates a change in the paramagnetic component of the chemical shift. The very nearly linear temperature dependencies ( $R > 0.998$  in all cases), both at low and high pH, suggest that no low-lying excited electronic states are populated in the temperature range observed and/or small zero-field splitting.

<sup>3</sup>For nomenclature please see the His structure scheme in the Methods section.

*Asp 156 assignments of Fe(II)SOD.* Both [<sup>2</sup>H] Asp Fe(II)SOD and [<sup>1</sup>H] Asp [<sup>2</sup>H] Fe(II)SOD were observed to identify the proton resonances of ligand Asp 156. None of the previously known resonances were absent from the <sup>1</sup>H NMR spectrum of [<sup>2</sup>H] Asp Fe(II)SOD. Instead, a broad loss of signal intensity, relative to spectra of unlabeled Fe(II)SOD, was observed in the 19–27 ppm range (data not shown), suggesting a broad Asp resonance or resonances in this region. This hypothesis was confirmed by the observation of [<sup>1</sup>H] Asp [<sup>2</sup>H] Fe(II)SOD (Figure 8). Two resonances, both with line widths of  $\sim 1500$  Hz, were detected at 26 and 22 ppm. We assign these resonances to the  $\beta$  protons of Asp 156, which are 4.4 and 4.5 Å from Fe(II).

*Non-ligand assignments of Fe(II)SOD.* NOEs from His 26 protons provide three non-ligand Fe(II)SOD assignments. We observe a NOESY cross peak between **k** and His 26  $\beta$  proton resonance **g** (data not shown). Resonance **k** is observed in <sup>15</sup>N-<sup>1</sup>H reverse INEPT spectra, which demonstrates that it is bonded to an N atom (data not shown). The NH proton of Tyr 27 is only 2.5 Å from the His 26  $\beta$  pro-R proton, so we assign **k** to the Tyr 27 NH proton. This proton is 8.0 Å from Fe, consistent with the narrow line width (80 Hz) of **k**. Since the pro-R His 26  $\beta$  proton is only 2.5 Å from the Tyr 27 NH proton while the pro-S proton is 3.8 Å away, and a NOESY cross peak between **k** and **g** but not **k** and **e** is observed, it can be concluded that **g** corresponds to the pro-R and **e** to the pro-S His 26  $\beta$  proton. We observe 1D NOEs from the His 26  $\delta 1$  proton (peak **a**) to **k**, **h** and **o** (Figure 3) and NOESY cross peaks have also been observed between **h** and **o** (Ming et al., 1994). The Trp 77  $\eta 2$  proton is 2.7 Å from the His 26  $\delta 1$  proton. We assign **h**, which has a line width of  $\sim 160$  Hz, to the Trp 77  $\eta 2$  proton which is 6.3 Å from Fe, and **o** (70 Hz) to the Trp 77  $\zeta 3$  proton (8.0 Å from Fe). Of the non-ligand peaks observed in the NOE difference spectrum of unlabeled Fe(II)SOD with **a** saturated, **k** and **o** probably arise from indirect saturation transfer through His 26  $\beta$  protons (peaks **e** and **g**), while **h** is a result of a NOE directly from the His 26  $\delta 1$  proton (peak **a**).

We assign resonance **y** to the methyl protons of Ala 161, based upon its integrated area of  $\sim 3$  protons and line width of 660 Hz at 30 °C (Figure 1). The Ala 161 methyl protons come as close to Fe as 4.0 Å as the group rotates. These are the only methyl protons within 7 Å of Fe(II) and therefore the only methyl

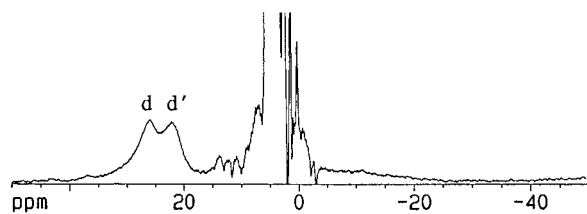


Figure 8.  $^1\text{H}$  NMR super-WEFT spectra (30 °C, 300 MHz) of  $[^1\text{H}]$  Asp  $[^2\text{H}]$  Fe(II)SOD in  $^2\text{H}_2\text{O}$ .

protons that could have proton resonance line widths of 660 Hz.

Beyond the ligand His ortho-like protons, the next closest proton to Fe(II) is a Trp 158  $\beta$  proton, at 3.7 Å. This was previously assigned to **I** (Ming et al., 1994) which has a line width of 90 Hz at 30 °C. We expect the resonance line width of this proton to be at least as broad as resonance **z** (1600 Hz at 30 °C, Figure 1), which is a non-ligand resonance as it is absent from  $^1\text{H}$  NMR spectra of  $[^1\text{H}]$  His  $[^2\text{H}]$  Fe(II)SOD and  $[^1\text{H}]$  Asp  $[^2\text{H}]$  Fe(II)SOD, and is present in  $[^2\text{H}]$  Asp Fe(II)SOD. The previous assignments of this and other Trp 158 protons to a spin system of narrow resonances (Ming et al., 1994) seem doubtful due to their proximity to Fe(II). Resonance **z** is the broadest observed non-ligand Fe(II)SOD resonance. While **z** may be that of a Trp 158  $\beta$  proton, it could also be that of either the Trp 122  $\eta_2$  or  $\zeta_2$  proton, which are 3.9 and 4.2 Å from Fe(II), respectively. The only other protons expected to be non-solvent exchangeable within 5 Å of Fe(II) are those of the Ala 161 methyl (to which we assign **y**) and the  $\epsilon_2$  Tyr 34 proton, which is 4.3 Å from Fe(II) according to the crystal structure. However, resonance **z** is absent from the spectra of  $[^1\text{H}]$  Tyr  $[^2\text{H}]$  Fe(II)SOD.

We tentatively assign a 450 Hz wide resonance (**I'**) at 13.5 ppm (at 30 °C) observed in the spectrum of  $[^1\text{H}]$  Tyr  $[^2\text{H}]$  FeSOD (data not shown) to the  $\epsilon_2$  Tyr 34 proton, or both Tyr 34  $\epsilon$  protons if the phenol group rotates rapidly. This resonance is highly overlapped by sharper resonances in spectra of unlabeled Fe(II)SOD.

**Ligand assignments of Fe(III)SOD.** The  $^1\text{H}$  NMR spectrum of Fe(III)SOD, unlike that of Fe(II)SOD, contains no sharp paramagnetically shifted resonances due to the longer spin relaxation time of high spin Fe(III) (Figure 9). Despite the breadth of the paramagnetically shifted features, some collective assignments are possible. The feature in the 80 to 120 ppm range is two or more resonances, all of which disappear upon transfer of the protein from  $^1\text{H}_2\text{O}$  into  $^2\text{H}_2\text{O}$ .

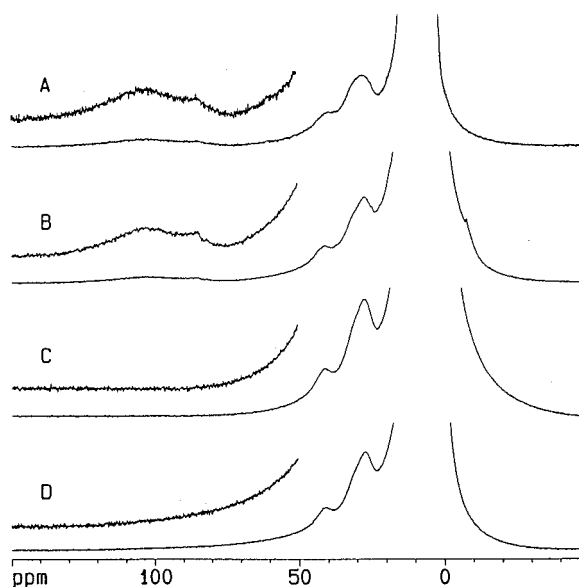


Figure 9.  $^1\text{H}$  NMR super-WEFT spectra (30 °C, 300 MHz) of  $[^1\text{H}]$  His  $[^2\text{H}]$  Fe(III)SOD in  $^1\text{H}_2\text{O}$  (A), unlabeled Fe(III)SOD in  $^1\text{H}_2\text{O}$  (B),  $[\epsilon_1, \delta_2\text{-}^2\text{H}]$  His Fe(III)SOD in  $^2\text{H}_2\text{O}$  (C), and unlabeled Fe(III)SOD in  $^2\text{H}_2\text{O}$  (D).

The resonances are therefore assigned to  $\delta_1$  protons of the ligand His residues. This is a common chemical shift range for high spin Fe(III) ligand His  $\delta_1$  protons, when His is  $\text{Ne}_2$  coordinated (Lauffer et al., 1983). In the 20–50 ppm range, the same pattern of resonances is seen in unlabeled Fe(III)SOD,  $[^1\text{H}]$  His  $[^2\text{H}]$  Fe(III)SOD, and  $[\epsilon_1, \delta_2\text{-}^2\text{H}]$  His Fe(III)SOD. These resonances are therefore those of  $\beta$  and/or  $\alpha$  His protons.

## Discussion

There have been relatively few studies of the Fe(II) sites of mononuclear non-heme, non-sulfur proteins. In the case of isopennicillin-N synthase (IPNS), signals were observed in a similar chemical shift range to the signals of FeSOD; however, few were assigned and the assignments were based on the assumption of three ligand His' (Ming et al., 1991), whereas crystal structures later revealed only two (Roach et al., 1995). Preliminary studies of FeSOD have also been reported (Ming et al., 1994; Renault and Morgenstren-Badarau, 1999). But the few proposed assignments were supported primarily by chemical shift comparisons with model compounds or/and NOESY spin systems. It is crucial to remember that NOESY cross peaks link protons near in space, but *not* necessarily

in the same side chain. Although specific labeling is tedious and sometimes costly, it provides essential definitive assignments and tests of proposals made based on NOESYs, etc. (Bertini et al., 1994; Bougault et al., 1998). Our revisions of the Fe(II)SOD assignments underline the subtlety of the factors that determine chemical shift. That chemical shift comparisons with models proved an insufficient basis for assignment is also informative, as it indicates that the protein active site engenders significantly different Fe(II) electronic and/or geometric structure from the models (Bertini et al., 1999). Comparison of enzyme chemical shifts and those of models may provide a sensitive probe of the faithfulness with which the model reproduces the enzyme, and will be very interesting to correlate with chemical activity.

The chemical shifts and line widths of paramagnetically shifted resonances reflect the electronic state of the metal ion, via the susceptibility tensor, and the covalency via hyperfine coupling. Both will contribute to the resonances of ligand protons but the latter is usually considered to be negligible for non-ligand protons. Although we have not separated the dipolar and hyperfine contributions, it is nonetheless interesting to compare the chemical shifts (and line widths) of our resonances with those assigned to analogous protons in other systems. FeSOD's Fe(II) might be most closely related to other sites from the group of mononuclear non-heme, non-sulfur Fe(II) proteins. Such Fe(II) binding sites with Asp and His ligation have been compared and found to display a common '2-His 1-carboxylate facial triad' motif which has been proposed to confer on these sites chemical versatility and O<sub>2</sub>-activating capability (Hegg and Que, 1997). The three empty or labile coordination sites of these enzymes were proposed to be crucial to the enzymes' ability to activate O<sub>2</sub> to attack substrate, by enabling them to bind both simultaneously, in contrast to heme proteins which can only coordinate one substrate or O<sub>2</sub> and therefore have been found to oxidize substrate via ferryl intermediates.

FeSOD has a fourth ligand, the axial His 26, which was proposed to limit FeSOD's activity to reacting with one substrate, O<sub>2</sub><sup>•-</sup>. Thus, the fourth ligand could be the cause of FeSOD's two-step reaction with one O<sub>2</sub><sup>•-</sup> in each step. In view of FeSOD's intermediacy between 2-His 1-carboxylate facial triad Fe proteins and hemes, it is interesting that FeSOD's axial His protons' chemical shifts are very similar to those of the axial ligand His of the cytochrome *c'* of *R. palustris*, as is the  $\delta 1$  proton chemical shift's temperature

dependence<sup>4</sup> (Bertini et al., 1998) (but see<sup>5</sup> (Bougault et al., 1998)). Moreover, His 26's  $\delta 1$  proton exchanges more slowly with solvent than those of either of the other ligand His', suggesting that His 26 is firmly tethered in place by hydrogen bonding or deeply buried. Thus, Fe(II)SOD's equatorial His<sub>2</sub> Asp triad reproduces at least some aspects of the electronic structure produced by a porphyrin. Moreover, this parallel holds for the catalytically active enzyme, since the reaction of Fe(II)SOD with O<sub>2</sub><sup>•-</sup> appears to proceed via an outer sphere mechanism (Whittaker and Solomon, 1988; Miller, 2001). Thus Fe(II)SOD may represent a case in which the electronic state and some of the reactive possibilities of a heme have been produced without recourse to a porphyrin, without committing as many coordination sites.

## Conclusions

We have assigned the <sup>1</sup>H NMR resonances of most Fe(II)SOD ligand protons, as well as some Fe(II)SOD non-ligand and Fe(III)SOD ligand protons. These are the most complete set of metal site <sup>1</sup>H NMR assignments yet obtained for a non-heme, non-sulfur, mononuclear Fe protein. Our results show the utility and feasibility of amino acid-specific isotopic labeling as well as the limitations of other techniques for obtaining paramagnetic metal site <sup>1</sup>H NMR assignments of proteins. We obtain chemical shifts that are significantly different than those observed in compounds thought to model the active site of Fe(II)SOD, and show that the axial His has chemical shifts very similar to those of an analogous ligand in a porphyrin system, suggesting possible functional parallels as well.

## Acknowledgements

We gratefully thank Dr. R. Trollard and C.I.L. for the gift of 1 l of <sup>2</sup>H<sub>2</sub>O. Acknowledgement is made to the donors of the Petroleum Research Fund, administered

<sup>4</sup>A Curie-type temperature dependence linear in 1/T is observed but the 1/T = 0 intercept of -9.3 deviates significantly from the anticipated diamagnetic chemical shift for a His  $\delta 1$  proton. The same behaviour occurs in *R. palustris* cytochrome *c'*. This has been variously ascribed to a combination of hyperfine and dipolar paramagnetic chemical shifting (Bertini et al., 1998) or to the contributions of zero-field splitting to the dipolar chemical shift (Bougault et al., 1998).

<sup>5</sup>Ferrous myoglobins' axial His ligand protons resonate closer to the values suggested by Ming's model compounds.

by the A.C.S., for partial support of this research under ACS-PRF 33266-AC4,3. A.-F.M. is pleased to thank N.I.H. for financial support (GM55210).

## References

- Balch, A.L., Chan, Y.-W., La Mar, G.N., Latos-Grazynski, L. and Renner, M.W. (1985) *Inorg. Chem.*, **24**, 1437–1443.
- Banci, L., Bertini, I., Luchinat, C. and Viezzoli, M.S. (1990) *Inorg. Chem.*, **29**, 1438–1440.
- Bertini, I., Dikiy, A., Luchinat, C., Macinai, R. and Viezzoli, M.S. (1998) *Inorg. Chem.*, **37**, 4814–4821.
- Bertini, I., Gori, G., Luchinat, C. and Villa, A.J. (1993a) *Biochemistry*, **32**, 776–783.
- Bertini, I., Jonsson, B.-H., Luchinat, C., Pierattelli, R. and Vila, A.J. (1994) *J. Magn. Reson.*, **B104**, 230–239.
- Bertini, I., Luchinat, C., Parigi, G. and Walker, F.A. (1999) *J. Biol. Inorg. Chem.*, **4**, 515–519.
- Bertini, I., Luchinat, C. and Tarchi, D. (1993b) *Chem. Phys. Lett.*, **203**, 445–449.
- Bertini, I., Turano, P. and Vila, A.J. (1993d) *Chem. Rev.*, **93**, 2833–2932.
- Bertini, L. and Luchinat, C. (1986) *NMR of Paramagnetic Molecules in Biological Systems*, Benjamin Cummings, New York, NY.
- Bougault, C.M., Dou, Y., Masao, I.-S., Langry, K.C., Smith, K.M. and La Mar, G.N. (1998) *J. Am. Chem. Soc.*, **120**, 2113–2123.
- Browne, D.T., Kenyon, G.L., Packer, E.L., Sternlicht, H. and Wilson, D.M.J. (1973) *J. Am. Chem. Soc.*, **95**, 1316–1323.
- Bull, C. and Fee, J.A. (1985) *J. Am. Chem. Soc.*, **107**, 3295–3304.
- Carlioz, A., Ludwig, M.L., Stallings, W.C., Fee, J.A., Steinman, H.M. and Touati, D. (1988) *J. Biol. Chem.*, **263**, 1555–1562.
- Cheng, H. and Markley, J.L. (1995) *Annu. Rev. Biophys. Biomol. Struct.*, **24**, 209–237.
- Fee, J.A., McClune, G.J., Lees, A.C., Zidovetzki, R. and Pecht, I. (1981) *Isr. J. Chem.*, **21**, 54–58.
- Feig, A.L. and Lippard, S.J. (1994) *Chem. Rev.*, **94**, 759–805.
- Goff, H. and La Mar, G.N. (1977) *J. Am. Chem. Soc.*, **99**, 6599–6605.
- Gueron, M. (1975) *J. Magn. Reson.*, **19**, 58–66.
- Hegg, E.L. and Que, L.J. (1997) *Eur. J. Biochem.*, **250**, 625–629.
- Hu, J.-S. and Redfield, A.G. (1993) *Biochemistry*, **32**, 6763–6772.
- Inubishi, T. and Becker, E.T. (1983) *J. Magn. Reson.*, **51**, 128–133.
- Lah, M.S., Dixon, M.M., Patridge, K.A., Stallings, W.C., Fee, J.A. and Ludwig, M.L. (1995) *Biochemistry*, **34**, 1646–1660.
- La Mar, G.N., Budd, D.L. and Goff, H. (1977) *Biochem. Biophys. Res. Commun.*, **77**, 104–110.
- La Mar, G.N., Horrocks, W.D., Jr. and Holm, R.H. (1973) *NMR of Paramagnetic Molecules*, Academic Press, New York, NY.
- Lauffer, R.B., Antanaitis, B.C., Aisen, P. and Que, L., Jr. (1983) *J. Biol. Chem.*, **258**, 14212–14218.
- Miller, A.-F. (2001) Fe-superoxide dismutase. In *Handbook of Metalloproteins*, Wieghardt, K., Huber, R., Poulos, T.L. and Messerschmidt, A., Eds. Wiley and Sons, New York, NY.
- Miller, A.-F. and Sorkin, D.L. (1997) *Commun. Mol. Cellular Biophys.*, **9**, 1–48.
- Ming, L.-J., Lynch, J.B., Holz, R.C. and Que, L., Jr. (1994) *Inorg. Chem.*, **33**, 83–87.
- Ming, L.-J., Que, L., Jr., Kriauciunas, A., Frolik, C.A. and Chen, V.J. (1991) *Biochemistry*, **30**, 11653–11659.
- Muchmore, D.C., McIntosh, L.P., Russell, C.B., Anderson, D.E. and Dahlquist, F.W. (1989) *Methods Enzymol.*, **177**, 44–73.
- Pappu, K. and Serpersu, E.H. (1994) *J. Magn. Reson.*, **B105**, 157–166.
- Parker, J. and Friesen, J.D. (1980) *Mol. Gen. Genet.*, **177**, 439–445.
- Qin, J., Delaglio, F., La Mar, G.N. and Bax, A. (1993) *J. Magn. Reson.*, **B102**, 332–336.
- Que, L., Jr. and Ho, R.Y.N. (1996) *Chem. Rev.*, **96**, 2607–2624.
- Redfield, A.G. and Gupta, R.K. (1971) *Cold Spring Harbor Symp. Quant. Biol.*, **36**, 541–550.
- Renault, J.P. and Morgenstren-Badarau, I. (1999) *Inorg. Chem.*, **38**, 614–615.
- Roach, P.L., Clifton, I.J., Fulop, V., Harlos, K., Barton, G.J., Hajdu, J., Andersson, I., Schofield, C.J. and Baldwin, J.E. (1995) *Nature*, **375**, 700–704.
- Sadek, M., Brownlee, R.T.C., Scrofolani, S.D.B. and Wedd, A.G. (1993) *J. Magn. Reson.*, **B101**, 309–314.
- Satterlee, J.D. (1986) *Ann. Rep. NMR Spectrosc.*, **17**, 79–178.
- Sorkin, D.L. and Miller, A.-F. (1997) *Biochemistry*, **36**, 4916–4924.
- Sorkin, D.L., Duong, D.K. and Miller, A.-F. (1997) *Biochemistry*, **36**, 8202–8208.
- Stallings, W.C., Metzger, A.L., Patridge, K.A., Fee, J.A. and Ludwig, M.L. (1991) *Free Rad. Res. Commun.*, **12–13**, 259–268.
- Thanabal, V. and La Mar, G.N. (1989) *Biochemistry*, **28**, 7038–7044.
- Tierney, D.L., Fee, J.A., Ludwig, M.L. and Penner-Hahn, J.E. (1995) *Biochemistry*, **34**, 1661–1668.
- Vance, C.K., Kang, Y.M. and Miller, A.-F. (1997) *J. Biomol. NMR*, **9**, 201–206.
- Vathyam, S., Byrd, R.A. and Miller, A.-F. (1999) *J. Biomol. NMR*, **14**, 293–294.
- Vathyam, S., Byrd, R.A. and Miller, A.-F. (2000) *Magn. Reson. Chem.*, **38**, 536–542.
- Vaughan, J.D., Mughrabi, Z. and Wu, E.C. (1970) *J. Org. Chem.*, **35**, 1141–1145.
- Weiss, M.A., Redfield, A.G. and Griffey, R.H. (1986) *Proc. Natl. Acad. Sci. USA*, **83**, 1325–1329.
- Whittaker, J.W. and Solomon, E.I. (1988) *J. Am. Chem. Soc.*, **110**, 5329–5339.
- Wu, F.-J. and Kurtz, D.M., Jr. (1989) *J. Am. Chem. Soc.*, **111**, 6563–6572.
- Wüthrich, K. (1969) *Proc. Natl. Acad. Sci. USA*, **63**, 1071–1078.